

## Status of the global $b \rightarrow s\ell^+\ell^-$ fits

---

**Bernat Capdevila**<sup>1,2,\*</sup>

<sup>1</sup>*DAMTP, University of Cambridge, Wilberforce Road, Cambridge, CB3 0WA, United Kingdom*

<sup>2</sup>*Department of Physics and IFAE, Universitat Autònoma de Barcelona, Edifici Ciències, Bellaterra, 08193, Barcelona, Spain*

*E-mail:* [bc593@cam.ac.uk](mailto:bc593@cam.ac.uk), [bcapdevila@ifae.es](mailto:bcapdevila@ifae.es)

The exploration of rare neutral current  $b \rightarrow s\ell^+\ell^-$  transitions is pivotal in testing the Standard Model (SM) and probing the presence of New Physics (NP) phenomena. This proceedings article offers an overview of recent developments in the examination of anomalies, deviations from SM predictions, in semi-leptonic  $B$  meson decays. It encompasses both experimental and theoretical aspects within the domain of global analyses of  $b \rightarrow s\ell^+\ell^-$  observables. We start by reviewing the current status of the experimental measurements for the key observables that define the decay modes included in global analyses. Subsequently, we delve into the determination of non-perturbative contributions, crucial for the computation of the amplitudes of the various  $b \rightarrow s\ell^+\ell^-$  modes. Our focus extends to recent advancements in local and non-local form factor calculations and their implications for SM predictions. This sets the stage for a detailed exploration of the outcomes from recent global analyses in the context of one-dimensional (1D) and two-dimensional (2D) fits. We underscore the importance of lepton flavour universality (LFU) throughout this discussion. Furthermore, we explore the interconnections between the tensions in  $b \rightarrow s\ell^+\ell^-$  data and the anomalies in charged current  $b \rightarrow c\ell\nu$  transitions, most notably in the  $R(D)$  and  $R(D^*)$  ratios. Lastly, we comment on the enhancement of  $b \rightarrow s\tau^+\tau^-$  processes that follows from general NP explanations of the  $R(D)$  and  $R(D^*)$  anomalies within the Standard Model Effective Theory (SMEFT), under current constraints.

*21st Conference on Flavour Physics and CP Violation (FPCP2023)*

*29 May - 2 June 2023*

*Institut de Physique des 2 Infinis (IP2I), Lyon, France*

---

\*Speaker

## 1. Introduction

The Cabibbo-Kobayashi-Maskawa (CKM) mechanism, a cornerstone of the SM of Particle Physics [1], was firmly established by the  $B$  factories BELLE [2] and BaBar [3] in the early 2000s, providing a theoretical model for flavour-changing quark transitions. Subsequently, the discovery of the Higgs boson [4, 5] in 2012 at CERN's Large Hadron Collider (LHC) [6, 7] marked the completion of the SM. Consequently, the focus of current research has shifted towards the quest for new particles and interactions beyond the SM.

The search for new particles can take place both directly, at high energies, and indirectly, at the low-energy precision frontier. Direct detection of new particles is a very well-defined concept, for which we have distilled over the years very refined analytic strategies for its categorisation. Indirect detection is more involved both statistically and theoretically, often requiring of very high precision measurements of observables designed as null-tests within a given theory, that without the contribution of the corresponding new effects could never be explained. However, it is worth noting that historically indirect discoveries often preceded direct observations. The existence of the charm quark,  $W$  boson, top quark, and even the Higgs boson were initially indicated through indirect measurements, including Fermi interactions, kaon mixing, and signatures in several electroweak precision observables.

In this context, semi-leptonic decays of  $B$  mesons emerge as valuable tools for indirect searches. These decays offer clean experimental signatures, manageable theoretical uncertainties, and suppressed rates, making them highly sensitive probes for NP. This proceedings article focuses on the anomalies observed in  $b \rightarrow s\ell^+\ell^-$  processes while also considering the implications of the tensions in  $b \rightarrow c\tau\nu$  modes.

On one hand,  $b \rightarrow c\ell\nu$  transitions constitute tree-level charged current processes. The most significant NP signatures in decays mediated by these quark-level transitions are found in the ratios of branching ratios,

$$R_{D^{(*)}} = \frac{\mathcal{B}(B \rightarrow D^{(*)}\tau\nu)}{\mathcal{B}(B \rightarrow D^{(*)}\ell\nu)}, \quad (1)$$

where  $\ell = \mu, e$ . These ratios offer insights into the LFU structure of the SM. Any significant deviation from the LFU expectation would provide a robust indicator of NP, as LFU is a fundamental accidental symmetry of the SM. On the experimental front, these ratios have unveiled a tension between their measurements, averaging those from BaBar [8, 9], Belle [10, 11, 12, 13, 14], and LHCb [15, 16, 17, 18], and their predictions within the SM. This tension has been quantified at approximately  $3\sigma$  level [19]<sup>1</sup>.

On the other hand,  $b \rightarrow s\ell^+\ell^-$  transitions represent flavour-changing neutral current processes generated only at the loop level in the SM. This makes these transitions exceptionally sensitive to a wide range of NP effects. Key decay channels in this context include processes like  $B \rightarrow K^{(*)}\mu^+\mu^-$ ,  $B_s \rightarrow \phi\mu^+\mu^-$  and  $B_s \rightarrow \mu^+\mu^-$ . Some of the most important and representative observables to characterise the dynamics of these decay channels include branching ratios, optimised angular observables ( $P_{1,2,3,4,5,6,8}^{(\prime)}$ ) for the decays  $B_{(s)} \rightarrow K^*(\phi)\mu^+\mu^-$  [26], and the LFU ratios:

$$R_{K^{(*)}} = \frac{\mathcal{B}(B \rightarrow K^{(*)}\mu^+\mu^-)}{\mathcal{B}(B \rightarrow K^{(*)}e^+e^-)}. \quad (2)$$

<sup>1</sup>The averaged SM prediction quoted by HFLAV is based on references such as [20, 21, 22, 23, 24, 25].

With the assumption that NP typically occurs at energy scales higher than that of  $B$  mesons, the theoretical framework employed for these analyses is the Weak Effective Theory (WET) [27, 28]. Within this framework, particles at or above the electroweak scale in the SM, such as the top quark,  $W$ ,  $Z$ , and the Higgs boson, as well as hypothetical NP fields, are integrated out. This approach enables the modelling of these transitions using an effective Hamiltonian and process-independent interactions. In this context, NP effects are encapsulated by the effective operators and associated coupling constants of the effective theory, either introducing structures absent within the SM or modifying the numerical values of Wilson coefficients relative to their SM predictions.

This proceedings article offers an overview of the current experimental and theoretical status of the anomalies in  $b \rightarrow s\ell^+\ell^-$ , as discussed in Section 2. Moving on to Section 3, it provides a summary of the most significant findings and conclusions from recent model-independent fits. In the subsequent section, Section 4, it explores the potential for combined explanations that address both the  $b \rightarrow s\ell^+\ell^-$  and  $b \rightarrow c\ell\nu$  anomalies simultaneously. The section concludes by offering insights into the importance of complementary signals in the form of processes involving  $b \rightarrow s\tau^+\tau^-$  transitions. And, finally, we conclude in Section 5.

## 2. Overview of the Experimental and Theoretical Status

Among the various tensions observed over the last decade in phenomena related to  $b \rightarrow s\ell^+\ell^-$  transitions, one of the most persistent tensions revolves around the optimised angular observable  $P'_5$  in the angular distribution of the four-body decay  $B \rightarrow K^*(\rightarrow K\pi)\mu^+\mu^-$ . This particular observable deserves an in-depth discussion due to its significance, and simultaneously, it provides a basis for discussing the status of form factors, both local and non-local.

The angular observable  $P'_5$  [29] was initially measured at LHCb [30] and subsequently at Belle [31, 32], ATLAS [33], and CMS [34]. The most recent SM prediction for this observable in the two most anomalous bins, as per the theoretical approach described in Ref. [35], is presented in Ref. [36]:

$$P'_{5 \text{ SM}} [4.0,6.0] = -0.72 \pm 0.08, \quad (3)$$

$$P'_{5 \text{ SM}} [6.0,8.0] = -0.81 \pm 0.08. \quad (4)$$

The theoretical framework mentioned above is characterised by its reliance on local form factor (FF) determinations based on theoretical data computed using light-cone sum rules (LCSRs) with  $B$ -meson light-cone distribution amplitudes (LCDAs) exclusively<sup>2</sup>. It then mitigates the impact of assumptions made during the LCSR calculations by breaking down the resulting FFs into soft FFs and factorisable power corrections. This is accomplished by leveraging the symmetries within the large recoil region [37], following the improved QCD factorisation (iQCdf) approach of Ref. [38]. Additionally, the framework introduces an uncertainty component related to non-local form factors, which are accounted for using calculations of the associated non-local correlator (see Eq. (8)) using  $B$ -meson LCSR [39] and appropriate parameterisations [38, 35].

<sup>2</sup>Form factor calculations based on light-meson LCDAs and/or combined fits with lattice data points are excluded from this approach.

For the local form factor input, the framework utilises the most recent calculations of  $B \rightarrow V$  FFs based on  $B$ -meson LCDAs, up to twist four for both two- and three-particle distributions. These are commonly known as the GKvD FFs [40]. Among the various sources of uncertainty, encompassing parametric uncertainties, soft FFs, factorisable power corrections, and non-local form factors, it is worth noting that the primary contributors are parametric errors (constituting approximately 30%) and factorisable power corrections (making up about 50%). Further details on each type of uncertainty can be found in Ref. [35].

Despite the use of new GKvD FFs, which reduced the baseline uncertainties associated with FFs with respect to previous FF calculations based on LCSRs with  $B$ -meson LCDAs [41], the influence of conservative factorisable power corrections estimates and a slight shift in the SM central value prediction towards experimental data has somewhat diminished the tension with data. Nevertheless, deviations between theory and experiment in these bins remain significant:

$$P'_{5 \text{ LHCb}}^{[4.0,6.0]} = -0.439 \pm 0.111 \pm 0.036 \quad (1.9\sigma), \quad (5)$$

$$P'_{5 \text{ LHCb}}^{[6.0,8.0]} = -0.583 \pm 0.090 \pm 0.030 \quad (1.9\sigma). \quad (6)$$

It is worth noting that the specific treatment of factorisable power corrections significantly impacts the uncertainty on  $P'_5$  predictions. Alternative scenarios, varying from a more comprehensive treatment of correlations among power corrections to a more skeptical approach with increased uncertainty, produce different levels of tension with data.

Non-local form factor contributions, often referred to as long-distance charm-loop effects, constitute another significant source of uncertainty. The amplitude for the decay  $B \rightarrow M\ell^+\ell^-$  follows this structure:

$$\mathcal{M}(B \rightarrow M\ell^+\ell^-) = \frac{G_F \alpha}{\sqrt{2}\pi} V_{tb} V_{ts}^* \left[ (\mathcal{A}_V^\mu + \mathcal{H}^\mu) \bar{u}_\ell \gamma_\mu \nu_\ell + \mathcal{A}_A^\mu \bar{u}_\ell \gamma_\mu \gamma_5 \nu_\ell \right], \quad (7)$$

with  $\mathcal{A}_V^\mu = -(2m_b q_\nu / q^2) C_7 \langle M | \bar{s} \sigma^{\mu\nu} P_R b | B \rangle + C_9 \langle M | \bar{s} \gamma^\mu P_L b | B \rangle$ ,  $\mathcal{A}_A^\mu = C_{10} \langle M | \bar{s} \gamma^\mu P_L b | B \rangle$  and

$$\mathcal{H}^\mu = \frac{-16i\pi^2}{q^2} \sum_{i=1,\dots,6,8} C_i \int dx^4 e^{iq \cdot x} \langle M | T \{ j_{\text{em}}^\mu(x), O_i(0) \} | B \rangle, \quad (8)$$

where we have assumed no right-handed currents,  $C_{7,9,10}$  are the Wilson coefficients of the effective Hamiltonian as defined in Eq. (12). The electromagnetic quark current is represented by  $j_{\text{em}}^\mu$ , and  $O_{i=1,\dots,6,8}$  ( $C_{i=1,\dots,6,8}$ ) stand for four-quark effective operators (Wilson coefficients) in the same effective Hamiltonian.

While local contributions from FFs are included in  $\mathcal{A}_{V,A}^\mu$ , non-local charm-quark loop contributions are part of the term  $\mathcal{H}^\mu$ . The challenge of distinguishing a NP contribution in  $C_7$  and / or  $C_9$  from a non-local contribution to  $\mathcal{H}^\mu$  is rooted in the fact that the non-local form factor is identically coupled to the leptonic vector current. This introduces an intrinsic uncertainty in detecting any NP signal in these two Wilson coefficients. Therefore, it is of paramount importance to accurately estimate the uncertainties stemming from the non-local form factor  $\mathcal{H}^\mu$ . Various approaches have been employed in the literature to model this non-local contribution:

- i) Using LCSRs to compute the leading one soft-gluon exchange [39]. This was further corroborated in [42] with the observation of a rather small NLO correction.

- ii) Utilising a dispersive representation by using data from the  $J/\Psi$  and  $\Psi(2S)$  peaks to determine the analytic structure and  $q^2$  dependence of the  $\mathcal{H}^\mu$  term [43]. A more recent and detailed analysis can be found in Ref. [44].
- iii) Employing a fit to the resonances (including their associated complex phases) to determine whether the tail of a resonance could explain the deviation in the anomalous bins [45].

On the experimental side, in assessing the tensions in the  $B^0 \rightarrow K^{*0}\mu^+\mu^-$  angular distribution (and  $P'_5$  in particular), it is important to also consider the tensions observed at Belle [31, 32], ATLAS [33], and CMS [34] regarding  $P'_5$ , as well as in the charged channel  $B^+ \rightarrow K^{*+}\ell^+\ell^-$ , as measured by LHCb in Ref. [46]. In the latter case, smaller tensions, at the level of  $1.1\sigma$  and  $1.6\sigma$ , have been observed (see Ref.[36]), further intensifying the tension in the anomalous bins. Section 3 is dedicated to exploring the implications of combining all data.

Branching ratios for various other  $b \rightarrow s\ell^+\ell^-$  modes also exhibit systematic and coherent tensions [47, 48, 49] when compared to the deviations observed in angular distributions. Furthermore, although there have been no recent experimental updates on the branching ratios of the  $B^{(0,+)} \rightarrow K^{(0,+)}\mu^+\mu^-$  modes, significant progress on the theoretical side has influenced the predictions of observables for the pseudoscalar channels. In particular, a recent lattice calculation of the  $B \rightarrow K$  form factors across the entire  $q^2$  range by the HPQCD collaboration [50] has greatly increased the precision of our computations for  $B^{(+,0)} \rightarrow K^{(+,0)}\mu^+\mu^-$  related observables. Consequently, the uncertainties in the branching ratios of these channels, particularly in the low- $q^2$  region, have been reduced from approximately 30% to about 10%, with no significant shifts in the central values. This improvement has resulted in tensions of about  $4\sigma$  in several  $q^2$  bins [36]:

$$\begin{aligned}
\mathcal{B}(B^+ \rightarrow K^+\mu^+\mu^-)_{\text{SM}}^{[1.1,2.0]} &= (0.33 \pm 0.03) \times 10^{-7}, \\
\mathcal{B}(B^+ \rightarrow K^+\mu^+\mu^-)_{\text{SM}}^{[4.0,5.0]} &= (0.37 \pm 0.03) \times 10^{-7}, \\
\mathcal{B}(B^+ \rightarrow K^+\mu^+\mu^-)_{\text{SM}}^{[5.0,6.0]} &= (0.37 \pm 0.03) \times 10^{-7}, \\
\mathcal{B}(B^+ \rightarrow K^+\mu^+\mu^-)_{\text{LHCb}}^{[1.1,2.0]} &= (0.21 \pm 0.02) \times 10^{-7} \quad (4.0\sigma), \\
\mathcal{B}(B^+ \rightarrow K^+\mu^+\mu^-)_{\text{LHCb}}^{[4.0,5.0]} &= (0.22 \pm 0.02) \times 10^{-7} \quad (4.4\sigma), \\
\mathcal{B}(B^+ \rightarrow K^+\mu^+\mu^-)_{\text{LHCb}}^{[5.0,6.0]} &= (0.23 \pm 0.02) \times 10^{-7} \quad (4.0\sigma).
\end{aligned} \tag{9}$$

In addition, the experimental combination for the branching ratio of the purely leptonic decay  $B_s \rightarrow \mu^+\mu^-$ , which includes the latest CMS measurement [51], is as follows [52]:

$$\mathcal{B}(B_s \rightarrow \mu^+\mu^-)^{\text{Exp. Av.}} = (3.52^{+0.32}_{-0.30}) \times 10^{-9}, \tag{10}$$

being compatible with its SM prediction at the level of  $1\sigma$ , depending on the value of  $V_{cb}$  used for the associated theoretical prediction.

Finally, with regard to LFU observables, the recent results from the LHCb collaboration for the ratios  $R_{K^{(*)}}$  in different bins of dilepton invariant mass, utilising  $9 \text{ fb}^{-1}$  dataset, indicate no

significant deviations from the SM expectations [53, 54]:

$$\begin{aligned}
R_{K^*_{\text{LHCb}}}^{[0.1,1.1]} &= 0.994^{+0.094}_{-0.087} \quad (-0.0\sigma), \\
R_{K_{\text{LHCb}}}^{[1.1,6]} &= 0.949^{+0.048}_{-0.047} \quad (+1.1\sigma), \\
R_{K^*_{\text{LHCb}}}^{[0.1,1.1]} &= 0.927^{+0.099}_{-0.093} \quad (+0.5\sigma), \\
R_{K^*_{\text{LHCb}}}^{[1.1,6]} &= 1.027^{+0.077}_{-0.073} \quad (-0.4\sigma).
\end{aligned} \tag{11}$$

In contrast to earlier measurements, these new results suggest that the dominant NP contribution needs to be LFU.

### 3. Overview $b \rightarrow s\ell^+\ell^-$ Global Fits

The effective Hamiltonian, valid below the EW scale and relevant for  $b \rightarrow s\ell^+\ell^-$ , can be written as [55, 28]

$$\mathcal{H}_{\text{eff}} = -\frac{4G_F}{\sqrt{2}} V_{tb} V_{ts}^* \sum_i C_i(\mu) O_i(\mu). \tag{12}$$

Here,  $G_F$  represents the Fermi constant, while  $V_{tb}$  and  $V_{ts}$  are CKM matrix elements. The coefficients  $C_i(\mu)$  are the Wilson coefficients that encode short-distance dynamics, and  $O_i(\mu)$  are the corresponding effective operators. The scale  $\mu$  is the renormalisation scale at which the Hamiltonian is evaluated.

In addition to the SM operators, the effective Hamiltonian may include operators representing structures not generated within the SM. These structures can involve, for instance, right-handed currents or scalar interactions, arising in various NP scenarios. The most relevant operators for the following discussion are:

$$\begin{aligned}
O_7^{(\prime)} &= (\bar{s}\sigma_{\mu\nu} P_{R(L)} b) F^{\mu\nu}, \\
O_{9\ell}^{(\prime)} &= (\bar{s}\gamma_\mu P_{L(R)} b) (\bar{\ell}\gamma^\mu \ell), \\
O_{10\ell}^{(\prime)} &= (\bar{s}\gamma_\mu P_{L(R)} b) (\bar{\ell}\gamma^\mu \gamma_5 \ell),
\end{aligned} \tag{13}$$

where colour indices have been actively omitted, and  $P_{L,R} = (1 \mp \gamma_5)/2$  represent the chirality projection operators. The tensor  $F^{\mu\nu} \equiv \partial^\mu A^\nu - \partial^\nu A^\mu$ , where  $A^\mu(x)$  is the photon field, is the electromagnetic field strength and  $\sigma^{\mu\nu} = \frac{i}{2}[\gamma^\mu, \gamma^\nu]$ , with  $\gamma^\mu$  the gamma matrices in four dimensions. Finally,  $b$  and  $s$  denote the quark fields, while  $\ell$  stands for the leptonic fields.

The Wilson coefficients corresponding to the most relevant operators within the effective Hamiltonian in Eq. 12 have the following values within the SM at the scale  $\mu_b = 4.8$  GeV [56, 57, 58, 59, 60]:

$$\begin{aligned}
C_7^{\text{eff}}(\mu_b) &= -0.2923, \\
C_9(\mu_b) &= +4.0749, \\
C_{10}(\mu_b) &= -4.3085.
\end{aligned} \tag{14}$$

Several research groups have conducted global fits involving various combinations of Wilson Coefficients [36, 61, 62, 63]. These fits include 1D, 2D, and multidimensional scenarios with up to

20 independent Wilson coefficients simultaneously. Notably, the NP scenario  $C_9^U$ , which represents an LFU contribution [64], i.e.,  $C_{9\mu}^{\text{NP}} = C_{9e}^{\text{NP}} \equiv C_9^U$ , has proven particularly effective in explaining observed deviations. This alignment gains significance in light of the new LHCb measurements of  $R_{K^{(*)}}$  and the CMS measurement of  $B_s \rightarrow \mu^+\mu^-$ . In this section, we will primarily focus on the results presented in Ref. [36] and later compare them with findings from other research groups. Table 1 provides a selection of preferred NP scenarios. The confidence region plots in Fig. 1

Scenario		Best-fit point	$1\sigma$	Pull <sub>SM</sub>	p-value
$b \rightarrow s\ell^+\ell^-$	$C_9^U$	-1.17	[-1.33, -1.00]	5.8	39.9 %
$b \rightarrow s\ell^+\ell^-$	$C_9^U$	-1.18	[-1.35, -1.00]	5.5	39.1 %
	$C_{10}^U$	+0.10	[-0.04, +0.23]		
$b \rightarrow s\ell^+\ell^-$	$C_{9\mu}^V = -C_{10\mu}^V$	-0.08	[-0.14, -0.02]	5.6	41.1 %
	$C_9^U$	-1.10	[-1.27, -0.91]		
$b \rightarrow s\ell^+\ell^- + R(D^{(*)})$	$C_{9\mu}^V = -C_{10\mu}^V$	-0.11	[-0.17, -0.05]	6.3	35.4 %
	$C_9^U$	-0.78	[-0.90, -0.66]		

**Table 1:** Most prominent scenarios that emerge from a global fit to  $b \rightarrow s\ell^+\ell^-$  data (see also [36, 65]).

depict the  $1\sigma$  and  $2\sigma$  contours for the 2D scenarios  $(C_9^U, C_{10}^U)$  and  $(C_{9\mu}^{\text{NP}}, C_{9e}^{\text{NP}})$ , illustrating regions constrained by the individual modes comprising the global fits, LFUV observables,  $b \rightarrow s\mu^+\mu^-$  modes, and the global fit.

In the  $(C_9^U, C_{10}^U)$  scenario, the grey contour, primarily reflecting constraints posed by  $\mathcal{B}(B_s \rightarrow \mu^+\mu^-)$  and  $\mathcal{B}(B \rightarrow X_s\ell^+\ell^-)$ , predominantly indicates consistency with  $C_{10}^U = 0$ . This alignment is consistent across all other modes included in the global fit and it can be attributed to the current global average of  $\mathcal{B}(B_s \rightarrow \mu^+\mu^-)$  being compatible with the corresponding SM estimate at the level of approximately  $1\sigma$ . Meanwhile, all constraints are consistent within  $1\sigma$  with a value of  $C_9^U \sim -1$ .

In the  $(C_{9\mu}^{\text{NP}}, C_{9e}^{\text{NP}})$  scenario, the impact of the new LHCb measurements of  $R_{K^{(*)}}$  is evident, leading to a consensus among all components of the global fit favouring a NP contribution suggesting  $C_{9\mu}^{\text{NP}} = C_{9e}^{\text{NP}}$ . This implies a strong signal of LFU NP associated with the semileptonic  $O_{9\ell}$  operator. The combination of  $b \rightarrow s\mu^+\mu^-$  modes cannot place any bounds on  $C_{9e}^{\text{NP}}$ , explaining why this region is unconstrained with respect to this axis in the plot.  $B \rightarrow K\ell^+\ell^-$  favours negative values for both  $C_{9\mu}^{\text{NP}}$  and  $C_{9e}^{\text{NP}}$  and is consistent with the relation  $C_{9\mu}^{\text{NP}} = C_{9e}^{\text{NP}}$  at  $1\sigma$ , mainly due to  $R_K$  being the only  $B \rightarrow K\ell^+\ell^-$  observable contributing to  $C_{9e}^{\text{NP}}$ . The  $B \rightarrow K^*\ell^+\ell^-$  observables also prefer negative values for both Wilson coefficients, with negligible correlation. The same applies to the  $B_s \rightarrow \phi\ell^+\ell^-$  mode, which is also compatible with all the other modes at the  $1\sigma$  level but with larger errors. The more complex NP scenario  $(C_{9\mu}^V = -C_{10\mu}^V, C_9^U)$  [64], apart from offering one of the best quality-of-fit perspectives, allows establishing a model-independent connection between charged and neutral anomalies, as we will explore in the next section. Figure 2 presents the corresponding preferred regions, and the corresponding numerical values are provided in Table 1.

Let us now compare the results of global  $b \rightarrow s\ell^+\ell^-$  fits from various groups:

- ABCDMN: M. Algueró, A. Biswas, B. Capdevila, S. Descotes-Genon, J. Matias, M. Novoa-Brunet [36].

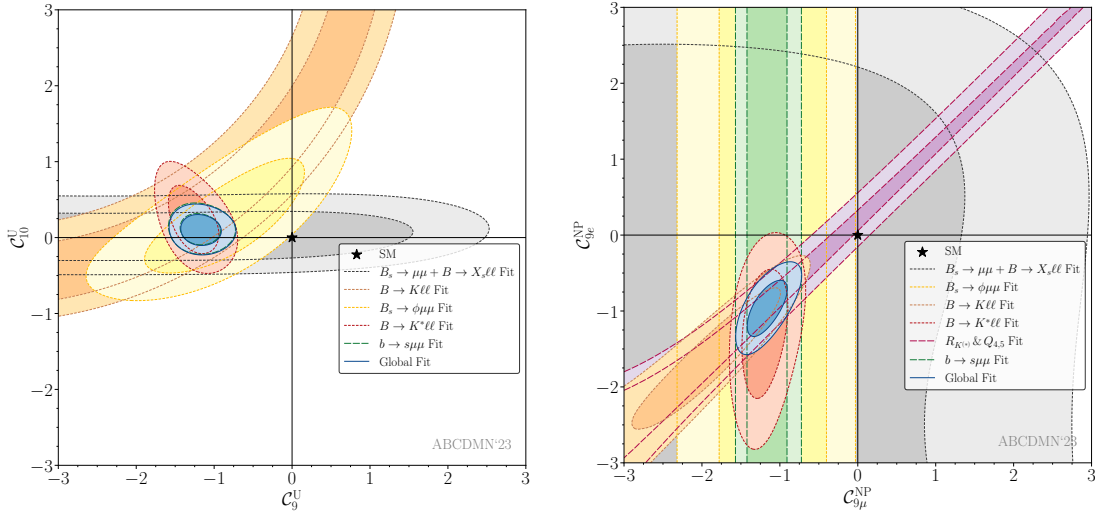


**Figure 1:**  $1\sigma$  (dark-shaded) and  $2\sigma$  (light-shaded) confidence regions for  $(C_9^U, C_{10}^U)$  (left) and  $(C_{9\mu}^{\text{NP}}, C_{9e}^{\text{NP}})$  scenarios (right). Distinct fits are performed separating each of the  $b \rightarrow s\ell^+\ell^-$  modes (short-dashed contours), the LFUV observables and the combined  $b \rightarrow s\mu^+\mu^-$  modes (long-dashed contours), and the global fit (solid contours). The colour code is provided in the individual captions. Notice that some fits (for instance the  $B \rightarrow K^{(*)}\ell^+\ell^-$  Fit(s) and the LFUV Fit) share a number of observables and thus are not completely uncorrelated.

- ▶ AS/GSSS: W. Altmannshofer, P. Stangl / A. Greljo, J. Salko, A. Smolkovic, P. Stang [61].
- ▶ CFFPSV: M. Ciuchini, M. Fedele, E. Franco, A. Paul, L. Silvestrini, M. Valli [62].
- ▶ HMMN: T. Hurth, F. Mahmoudi, D. Martínez-Santos, S. Neshatpour [63, 66].

These collaborations employ various statistical methods, FF choices, and assumptions about non-perturbative effects. For an in-depth review of their different approaches, readers are referred to Refs. [67, 68]. CFFPSV uses two distinct methods, namely, the Phenomenological Model Driven (PMD) and Phenomenological Data Driven (PDD) approaches. In the PMD approach, existing LCSR estimates are leveraged to constrain their proposed polynomial parametrisation in  $q^2$  for the non-local form factors. They then adjust the parameters of this parametrisation to the  $B \rightarrow K^*\mu^+\mu^-$  angular distributions while adhering to these constraints. In contrast, the PDD approach allows all parameters of their polynomial parametrisation to float freely without constraint and fits them to the available data.

Notably, as depicted in Fig. 3, despite the diverse methodologies pursued, a substantial level of agreement is evident when comparing the results within the  $(C_{9\mu}^{\text{NP}}, C_{10\mu}^{\text{NP}})$  plane. This convergence underscores the robustness and maturity achieved in analysing  $b \rightarrow s\ell^+\ell^-$  data, which is a pivotal conclusion drawn from the current status of  $b \rightarrow s\ell^+\ell^-$  analyses. However, one approach stands out for its significant disagreement with the others: the PDD approach from the CFFPSV group. This discrepancy arises from the very large number of free parameters, which allow it to absorb a large part of any potential NP effects. While the strategies adopted by the ABCDMN and HMMN collaborations share substantial similarities, particularly in terms of including all available data on meson decays, the AS/GSSS approach differs in that it does not incorporate measurements within

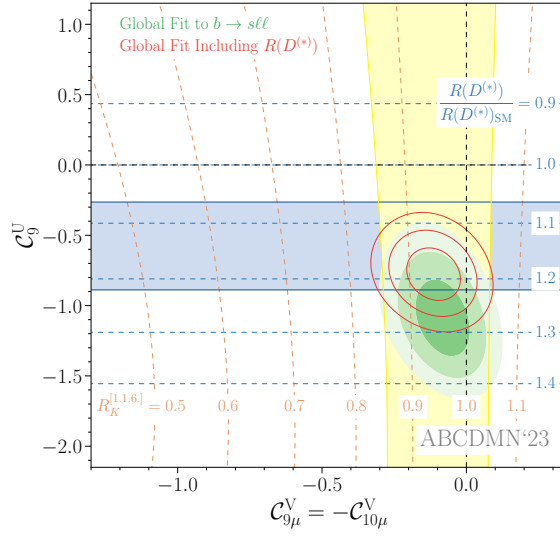


**Figure 2:** Preferred regions at the  $1\sigma$ ,  $2\sigma$  and  $3\sigma$  level (green) in the  $(C_{9\mu}^V = -C_{10\mu}^V, C_9^U)$  plane from  $b \rightarrow s\ell^+\ell^-$  data. The red contour lines show the corresponding regions once  $R_{D^{(*)}}$  is included (for a NP scale  $\Lambda = 2$  TeV). The horizontal blue (vertical yellow) band is consistent with  $R_{D^{(*)}}$  ( $R_K$ ) at the  $2\sigma$  level and the contour lines show the predicted values for these ratios.

the kinematic regime where  $q^2 > 6 \text{ GeV}^2$ . Inclusion of such data could align their results more closely with those of both the ABCDMN and HMMN collaborations. Regarding the latter two, their level of agreement and consistency is notably high, attributed to their similar data selection and treatment of non-perturbative effects. The key distinction is that the ABCDMN collaboration primarily focuses on meson decays, while HMMN also includes the baryonic decay  $\Lambda_b \rightarrow \Lambda\mu^+\mu^-$ .

While not shown in Fig. 3, it is worth briefly mentioning the results from the GRvDV group (N. Gubernari, M. Reboud, D. van Dyk, J. Virto) [69]. Their framework is based on a simultaneous Bayesian fit of all non-perturbative parameters, including the coefficients of the parameterisations for both local and non-local form factors, along with the NP contributions to the relevant Wilson Coefficients. To control the uncertainty in the parametrisation of non-local form factors, GRvDV derived unitarity bounds for the aforementioned parametrisation based on the analytic structure of the correlator  $\mathcal{H}^\mu$  in Eq. (8). Due to the technical complexity of their framework, which involves fitting a large number of free parameters, they currently only present dedicated fits to  $B \rightarrow K^*\mu^+\mu^-$ ,  $B \rightarrow K\mu^+\mu^-$ , and  $B_s \rightarrow \phi\mu^+\mu^-$  in Ref. [69]. However, the relevance of their results, particularly concerning their determinations of local and non-local form factors using both theoretical and experimental data under suitable unitarity bounds, deserves special recognition. We look forward to future results obtained from such a framework combining all the different channels into a fully-fleshed  $b \rightarrow s\ell^+\ell^-$  global fit.

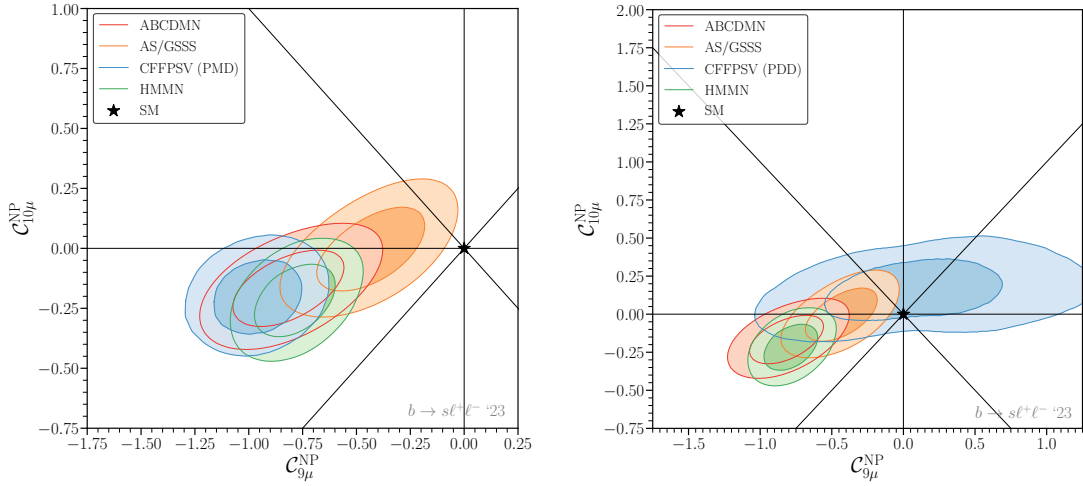


**Figure 3:** Comparison of the results of the global fits of the different collaborations in the  $C_{9\mu}^{\text{NP}}-C_{10\mu}^{\text{NP}}$  plane.

#### 4. Correlations between the $b \rightarrow s\ell^+\ell^-$ and $b \rightarrow c\ell\nu$ Anomalies: $b \rightarrow s\tau^+\tau^-$ enhancement

To complement the EFT analysis discussed earlier, we now shift our focus to the NP interpretation of scenario ( $C_{9\mu}^{\text{V}} = -C_{10\mu}^{\text{V}}, C_9^{\text{U}}$ ). Indeed, this scenario allows for a model-independent connection between the anomalies in  $b \rightarrow s\ell^+\ell^-$  and those in  $b \rightarrow c\ell\nu$ . This correlation arises naturally within the SMEFT due to the presence of two four-fermion operators that generate the relevant semileptonic quark currents [70, 71]:

$$\mathcal{O}_{ijkl}^{(1)} = [\bar{Q}_i\gamma_\mu Q_j][\bar{L}_k\gamma^\mu L_l], \quad (15)$$

$$\mathcal{O}_{ijkl}^{(3)} = [\bar{Q}_i\gamma_\mu\sigma^I Q_j][\bar{L}_k\gamma^\mu\sigma^I L_l]. \quad (16)$$

Allowing CKM favoured terms only and excluding currents that are not allowed by phase space, the SMEFT operators  $\mathcal{O}_{23kl}^{(1,3)}$  generate the following currents [71]:

$$\begin{aligned} \mathcal{C}_{23kl}^{(1)}\mathcal{O}_{23kl}^{(1)} = \mathcal{C}_{23kl}^{(1)} & \left[ (\bar{s}_L\gamma_\mu b_L)(\bar{\ell}_L\gamma^\mu \ell_L) + (\bar{s}_L\gamma_\mu b_L)(\bar{\nu}_{\ell k}\gamma^\mu \nu_{\ell l}) \right. \\ & \left. + V_{tb}V_{cs} \left( (\bar{c}_L\gamma_\mu t_L)(\bar{\ell}_L\gamma^\mu \ell_L) + (\bar{c}_L\gamma_\mu t_L)(\bar{\nu}_{\ell k}\gamma^\mu \nu_{\ell l}) \right) \right], \end{aligned} \quad (17)$$

$$\begin{aligned} \mathcal{C}_{23kl}^{(3)}\mathcal{O}_{23kl}^{(3)} = \mathcal{C}_{23kl}^{(3)} & \left[ (\bar{s}_L\gamma_\mu b_L)(\bar{\ell}_L\gamma^\mu \ell_L) - (\bar{s}_L\gamma_\mu b_L)(\bar{\nu}_{\ell k}\gamma^\mu \nu_{\ell l}) \right. \\ & \left. + 2V_{cs}(\bar{c}_L\gamma_\mu b_L)(\bar{\ell}_L\gamma^\mu \nu_{\ell l}) \right. \\ & \left. + V_{tb}V_{cs} \left( -(\bar{c}_L\gamma_\mu t_L)(\bar{\ell}_L\gamma^\mu \ell_L) + (\bar{c}_L\gamma_\mu t_L)(\bar{\nu}_{\ell k}\gamma^\mu \nu_{\ell l}) \right) \right]. \end{aligned} \quad (18)$$

However, it is important to note from Eqs. (17)-(18) that these operators also lead to terms that contribute to other processes like  $B \rightarrow K^{(*)}\nu\nu$  and  $t \rightarrow c$  transitions. Although the constraints on  $t \rightarrow c$  transitions are still preliminary and do not pose strong limitations, and hence can be safely disregarded from here on,  $B \rightarrow K^{(*)}\nu\nu$  processes provide stringent bounds on NP<sup>3</sup>.

<sup>3</sup>Note the recent results presented by the BELLE II collaboration with an excess in  $B^+ \rightarrow K^+\nu\nu$  [72], which could be related to the  $B$  anomalies discussed here. However, the differential distribution seems to prefer light NP.

To avoid generating these undesired currents we restrict our analysis by imposing  $C^{(1)} = C^{(3)}$ . Under this condition, considering second and third-generation leptons, the generated currents by the four-fermion SMEFT operators discussed above are:

$$C_{2322}^{(1)}\mathcal{O}_{2322}^{(1)} + C_{2322}^{(3)}\mathcal{O}_{2322}^{(3)} = C_{2322}^{(1=3)} \left[ 2(\bar{s}_L\gamma_\mu b_L)(\bar{\mu}_L\gamma^\mu\mu_L) + 2V_{cs}(\bar{c}_L\gamma_\mu b_L)(\bar{\mu}_L\gamma^\mu\nu_\mu) \right], \quad (19)$$

$$C_{2333}^{(1)}\mathcal{O}_{2333}^{(1)} + C_{2333}^{(3)}\mathcal{O}_{2333}^{(3)} = C_{2333}^{(1=3)} \left[ 2(\bar{s}_L\gamma_\mu b_L)(\bar{\tau}_L\gamma^\mu\tau_L) + 2V_{cs}(\bar{c}_L\gamma_\mu b_L)(\bar{\tau}_L\gamma^\mu\nu_\tau) \right]. \quad (20)$$

In particular, as shown on the right-hand side of Eq. (20), these structures lead to contributions to the left-handed vector operator:

$$\mathcal{O}_{V_L} = (\bar{c}_L\gamma_\mu b_L)(\bar{\tau}_L\gamma^\mu\nu_\tau), \quad (21)$$

which is the favoured NP explanation for the  $R(D^{(*)})$  anomalies, as suggested by the global EFT fits to  $b \rightarrow c\ell\nu$  data [73]. Notice that the NP scenario where the  $R(D^{(*)})$  anomalies are explained through the  $\mathcal{O}_{V_L}$  operator, since this amounts to a redefinition of the Fermi constant, it predicts:

$$R_{J/\psi}/R_{J/\psi}^{\text{SM}} = R_D/R_D^{\text{SM}} = R_{D^*}/R_{D^*}^{\text{SM}} \equiv R_X/R_X^{\text{SM}}, \quad (22)$$

agreeing well with the current measurements within uncertainties.

Additionally, it is worth noting that the same SMEFT NP scenario, which provides an explanation for the  $R(D^{(*)})$  anomalies, also results in indirect NP contributions to processes involving  $b \rightarrow s\tau^+\tau^-$  transitions through the operator  $(\bar{s}_L\gamma_\mu b_L)(\bar{\tau}_L\gamma^\mu\tau_L)$ . This operator, within the framework of the WET Hamiltonian for  $b \rightarrow s\tau^+\tau^-$  transitions, emerges in the NP scenario where  $C_{9\tau}^{\text{NP}} = -C_{10\tau}^{\text{NP}}$  [71]. Consequently, NP effects in  $R_X/R_X^{\text{SM}}$  naturally lead to NP contributions in  $b \rightarrow s\tau^+\tau^-$  processes through

$$C_{9\tau(10\tau)}^{\text{NP}} \approx C_{9(10)}^{\text{SM}} - (+)\Delta, \quad (23)$$

with

$$\Delta = \frac{2\pi}{\alpha} \frac{V_{cb}}{V_{tb}V_{ts}^*} \left( \sqrt{\frac{R_X}{R_X^{\text{SM}}}} - 1 \right). \quad (24)$$

We want to emphasise that the factor multiplying the bracket in Eq. (24) is remarkably large, approximately 860. Using the 2019 HFLAV averages for  $R_{D^{(*)}}$  (which have not significantly changed with the most recent results), we calculate a substantial positive (or negative) NP contribution to the Wilson coefficient  $C_{9\tau}^{\text{NP}}$  (or  $C_{10\tau}^{\text{NP}}$ ). This contribution is parameterised by  $\Delta = O(50)$ . It is worth noting that before the Belle collaboration's update of  $R_{D^{(*)}}$  in early 2019, the value of  $\Delta$  was around  $O(100)$ . This sizable contribution completely dominates the SM contribution to these Wilson coefficients, leading to a significant enhancement of branching ratios for processes like  $B_s \rightarrow \tau^+\tau^-$ ,  $B \rightarrow K^{(*)}\tau^+\tau^-$ , and  $B_s \rightarrow \phi\tau^+\tau^-$ , as illustrated in Fig. 4. The substantial enhancement of  $b \rightarrow s\tau^+\tau^-$  modes can be attributed to the fact that the NP effects in  $b \rightarrow c\tau\nu$  required to explain  $R(D^{(*)})$  is approximately 10% of the SM operator. This, being a tree-level process, has a profound impact, leading to a correspondingly significant effect on  $b \rightarrow s\tau^+\tau^-$  processes.

At the same time, within the framework of the WET, the condition  $C_{9\tau}^{\text{NP}} = -C_{10\tau}^{\text{NP}}$  leads to a mixing effect with the four-fermion operators  $\mathcal{O}_{9\ell}$  (where  $\ell = e$  or  $\mu$ ) within the effective theory.

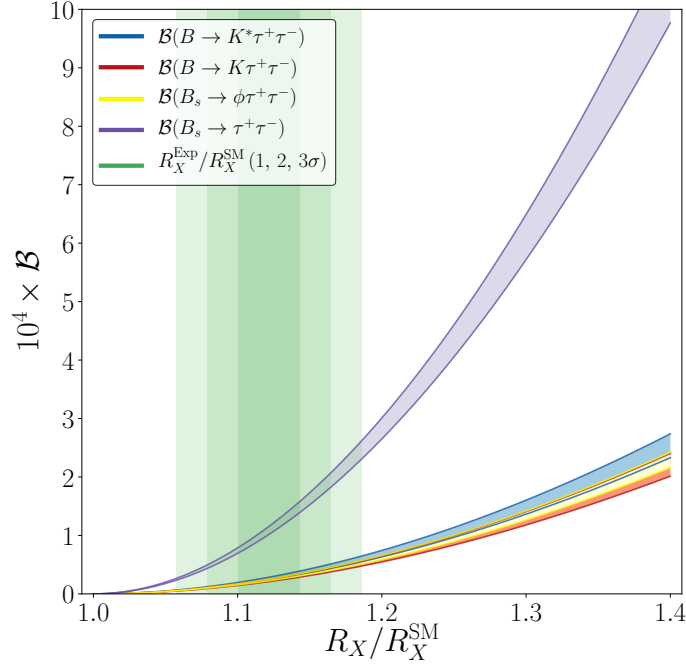


**Figure 4:** Predictions of the branching ratios of the  $b \rightarrow s\tau^+\tau^-$  processes (including uncertainties) as a function of  $R_X/R_X^{\text{SM}}$ . The green bands indicate the current experimental ranges for  $R_X/R_X^{\text{SM}}$ , obtained by performing the weighted average of  $R_D$ ,  $R_{D^*}$  and  $R_{J/\psi}$  without taking into account correlations.

This mixing generates an LFU effect in  $C_9^{\text{U}}$ , i.e the LFU part of scenario ( $C_{9\mu}^{\text{V}} = -C_{10\mu}^{\text{V}}, C_9^{\text{U}}$ ), at  $\mu = m_b$  [74]

$$C_9^{\text{U}} \simeq 7.5 \left( 1 - \sqrt{\frac{R(D^{(*)})}{R(D^{(*)})_{\text{SM}}}} \right) \left( 1 + \frac{\log \frac{\Lambda^2}{1\text{TeV}^2}}{10.5} \right), \quad (25)$$

assuming large flavour-violating (i.e. non-aligned) couplings. Using a combination of  $D$  and  $D^*$  data, this results in  $R(D^{(*)})_{\text{exp}}/R(D^{(*)})_{\text{SM}} = 1.142 \pm 0.039$ , which implies  $C_9^{\text{U}} \simeq -0.58$ , assuming a NP scale  $\Lambda$  of 2 TeV [71, 75].

On the other hand, the first term in Eq. (19) generates a NP effect only in  $b \rightarrow s\mu^+\mu^-$  transitions, representing a purely LFUV effect. Notably, since  $(\bar{s}_L\gamma_\mu b_L)(\bar{\mu}_L\gamma^\mu\mu_L)$  contains a left-handed lepton current, it gives rise to a  $C_9 = -C_{10}$  structure. Consequently, this term can be identified as the source of the LFUV component,  $C_{9\mu}^{\text{V}} = -C_{10\mu}^{\text{V}}$ , within the scenario ( $C_{9\mu}^{\text{V}} = -C_{10\mu}^{\text{V}}, C_9^{\text{U}}$ ).

Finally, one more observation is worth noting. If we assume that the same mechanism that correlates  $b \rightarrow c\tau\nu$  and  $b \rightarrow s\tau^+\tau^-$  transitions extends to muons, as suggested by the structure of Eq. (19), we also obtain a correlation between  $b \rightarrow s\mu^+\mu^-$  and  $b \rightarrow c\mu\nu$  transitions. However, the  $O(20\%)$  shift required in  $C_{9\mu}^{\text{NP}}$  to describe  $b \rightarrow s\mu^+\mu^-$  data [76] results in a very small positive  $\Delta$  and only a minimal decrease in  $b \rightarrow c\mu\nu$  decay rates compared to the Standard Model, by an insignificant amount of only a few parts per thousand. Therefore, there would be no measurable differences between electron and muon semileptonic decays.

This entire correlation scheme among the different anomalies in  $b \rightarrow c\ell\nu$  and  $b \rightarrow s\mu^+\mu^-$ , along with the prediction of the inevitable consequence of significantly enhanced  $b \rightarrow s\tau^+\tau^-$  branching ratios, presents us with a clear testing ground. If a common NP explanation for the anomalies in  $b \rightarrow c\ell\nu$  and  $b \rightarrow s\mu^+\mu^-$  at very high energy scales, resulting in contact interactions, such as those described in Eqs. (15)-(16) in the form of four-fermion operators within the SMEFT, exists, then we should necessarily observe  $b \rightarrow s\tau^+\tau^-$  branching ratios approximately two orders of magnitude larger than what the SM predicts.

## 5. Conclusions

Semi-leptonic  $B$  decays serve as valuable probes of the SM. They are characterised by manageable theoretical uncertainties, distinct experimental signatures, and sensitivity to NP effects due to their suppressed rates. In this proceedings, we provide an overview of the current status of the  $b \rightarrow s\ell^+\ell^-$  anomalies, the global fitting analyses performed to explore their implications for NP, and their connections with other anomalous channels.

The  $b \rightarrow s\ell^+\ell^-$  transitions involve flavour-changing neutral currents, which are only mediated at the loop level in the SM. Consequently, they are highly sensitive to small NP effects. The main drivers of these anomalies are [36]:

- i) Deviations in  $\mathcal{B}(B^+ \rightarrow K^+\mu^+\mu^-)$ , with discrepancies in several bins at a significance level of  $4\sigma$ , and a systematic trend observed in other branching ratios, although less pronounced.
- ii)  $P'_5$ , which exhibits the most persistent tension, deviating by approximately  $2\sigma$  (considering only the neutral channel) in the two anomalous bins, supported by measurements of the charged mode.
- iii) Discrepancies in the branching ratio and angular observables in  $B_s \rightarrow \phi\mu^+\mu^-$ , depending on the choice of FFs used.

Crucially, these deviations from the SM collectively form a consistent picture. They can be explained by a simple NP scenario without violating bounds from other observables. Notably, the two leading scenarios, which take into account the updated measurements of  $R_K$  and  $R_{K^*}$ , are  $C_9^U$  and  $(C_{9\mu}^V = -C_{10\mu}^V, C_9^U)$  with significance levels of  $5.8\sigma$  and  $6.3\sigma$  (if  $R(D^{(*)})$  is included), respectively [36]. This suggests the presence of NP with a magnitude of approximately 20% compared to the SM.

On the other hand,  $b \rightarrow c\ell\nu$  transitions, being tree-level mediated charged current processes, exhibit substantial decay rates. The ratios  $R(D)$  and  $R(D^*)$  indicate a departure from the LFU expectation. The solution to the  $R(D)$  and  $R(D^*)$  anomalies through a left-handed vector current also provides the most straightforward possibility for a unified explanation. In the promising scenario  $(C_{9\mu}^V = -C_{10\mu}^V, C_9^U)$ ,  $C_9^U$  is attributed to a tau-loop, while  $C_{9\mu}^V = -C_{10\mu}^V$  arises from a direct tree-level effect.

Moreover, this scenario predicts measurable rates for  $b \rightarrow s\tau^+\tau^-$  processes, which are linked to the magnitude of  $R(D^{(*)})$  and  $C_9^U$ . Providing an optimal testing ground for the consistency of a possible NP explanation for the anomalies.

## Acknowledgments

The work of B.C. is supported by the Margarita Salas postdoctoral program funded by the European Union-NextGenerationEU. B.C. also thanks the Cambridge Pheno Working Group for helpful discussions and M. Algueró, A. Biswas, S. Descotes-Genon, J. Matias and M. Novoa-Brunet for years of fruitful collaboration.

## References

- [1] Makoto Kobayashi and Toshihide Maskawa. “CP Violation in the Renormalizable Theory of Weak Interaction”. In: *Prog. Theor. Phys.* 49 (1973), pp. 652–657. DOI: [10.1143/PTP.49.652](https://doi.org/10.1143/PTP.49.652).
- [2] A. Abashian et al. “The Belle Detector”. In: *Nucl. Instrum. Meth. A* 479 (2002), pp. 117–232. DOI: [10.1016/S0168-9002\(01\)02013-7](https://doi.org/10.1016/S0168-9002(01)02013-7).
- [3] Bernard Aubert et al. “The BaBar detector”. In: *Nucl. Instrum. Meth. A* 479 (2002), pp. 1–116. DOI: [10.1016/S0168-9002\(01\)02012-5](https://doi.org/10.1016/S0168-9002(01)02012-5). arXiv: [hep-ex/0105044](https://arxiv.org/abs/hep-ex/0105044).
- [4] Peter W. Higgs. “Broken symmetries, massless particles and gauge fields”. In: *Phys. Lett.* 12 (1964), pp. 132–133. DOI: [10.1016/0031-9163\(64\)91136-9](https://doi.org/10.1016/0031-9163(64)91136-9).
- [5] F. Englert and R. Brout. “Broken Symmetry and the Mass of Gauge Vector Mesons”. In: *Phys. Rev. Lett.* 13 (1964). Ed. by J. C. Taylor, pp. 321–323. DOI: [10.1103/PhysRevLett.13.321](https://doi.org/10.1103/PhysRevLett.13.321).
- [6] Georges Aad et al. “Observation of a new particle in the search for the Standard Model Higgs boson with the ATLAS detector at the LHC”. In: *Phys. Lett. B* 716 (2012), pp. 1–29. DOI: [10.1016/j.physletb.2012.08.020](https://doi.org/10.1016/j.physletb.2012.08.020). arXiv: [1207.7214](https://arxiv.org/abs/1207.7214) [[hep-ex](#)].
- [7] Serguei Chatrchyan et al. “Observation of a New Boson at a Mass of 125 GeV with the CMS Experiment at the LHC”. In: *Phys. Lett. B* 716 (2012), pp. 30–61. DOI: [10.1016/j.physletb.2012.08.021](https://doi.org/10.1016/j.physletb.2012.08.021). arXiv: [1207.7235](https://arxiv.org/abs/1207.7235) [[hep-ex](#)].
- [8] J. P. Lees et al. “Evidence for an excess of  $\bar{B} \rightarrow D^{(*)}\tau^-\bar{\nu}_\tau$  decays”. In: *Phys. Rev. Lett.* 109 (2012), p. 101802. DOI: [10.1103/PhysRevLett.109.101802](https://doi.org/10.1103/PhysRevLett.109.101802). arXiv: [1205.5442](https://arxiv.org/abs/1205.5442) [[hep-ex](#)].
- [9] J. P. Lees et al. “Measurement of an Excess of  $\bar{B} \rightarrow D^{(*)}\tau^-\bar{\nu}_\tau$  Decays and Implications for Charged Higgs Bosons”. In: *Phys. Rev. D* 88.7 (2013), p. 072012. DOI: [10.1103/PhysRevD.88.072012](https://doi.org/10.1103/PhysRevD.88.072012). arXiv: [1303.0571](https://arxiv.org/abs/1303.0571) [[hep-ex](#)].
- [10] M. Huschle et al. “Measurement of the branching ratio of  $\bar{B} \rightarrow D^{(*)}\tau^-\bar{\nu}_\tau$  relative to  $\bar{B} \rightarrow D^{(*)}\ell^-\bar{\nu}_\ell$  decays with hadronic tagging at Belle”. In: *Phys. Rev. D* 92.7 (2015), p. 072014. DOI: [10.1103/PhysRevD.92.072014](https://doi.org/10.1103/PhysRevD.92.072014). arXiv: [1507.03233](https://arxiv.org/abs/1507.03233) [[hep-ex](#)].
- [11] Y. Sato et al. “Measurement of the branching ratio of  $\bar{B}^0 \rightarrow D^{*+}\tau^-\bar{\nu}_\tau$  relative to  $\bar{B}^0 \rightarrow D^{*+}\ell^-\bar{\nu}_\ell$  decays with a semileptonic tagging method”. In: *Phys. Rev. D* 94.7 (2016), p. 072007. DOI: [10.1103/PhysRevD.94.072007](https://doi.org/10.1103/PhysRevD.94.072007). arXiv: [1607.07923](https://arxiv.org/abs/1607.07923) [[hep-ex](#)].
- [12] S. Hirose et al. “Measurement of the  $\tau$  lepton polarization and  $R(D^*)$  in the decay  $\bar{B} \rightarrow D^*\tau^-\bar{\nu}_\tau$ ”. In: *Phys. Rev. Lett.* 118.21 (2017), p. 211801. DOI: [10.1103/PhysRevLett.118.211801](https://doi.org/10.1103/PhysRevLett.118.211801). arXiv: [1612.00529](https://arxiv.org/abs/1612.00529) [[hep-ex](#)].

- [13] S. Hirose et al. “Measurement of the  $\tau$  lepton polarization and  $R(D^*)$  in the decay  $\bar{B} \rightarrow D^*\tau^-\bar{\nu}_\tau$  with one-prong hadronic  $\tau$  decays at Belle”. In: *Phys. Rev. D* 97.1 (2018), p. 012004. DOI: [10.1103/PhysRevD.97.012004](https://doi.org/10.1103/PhysRevD.97.012004). arXiv: [1709.00129](https://arxiv.org/abs/1709.00129) [hep-ex].
- [14] G. Caria et al. “Measurement of  $\mathcal{R}(D)$  and  $\mathcal{R}(D^*)$  with a semileptonic tagging method”. In: *Phys. Rev. Lett.* 124.16 (2020), p. 161803. DOI: [10.1103/PhysRevLett.124.161803](https://doi.org/10.1103/PhysRevLett.124.161803). arXiv: [1910.05864](https://arxiv.org/abs/1910.05864) [hep-ex].
- [15] Roel Aaij et al. “Measurement of the ratio of branching fractions  $\mathcal{B}(\bar{B}^0 \rightarrow D^{*+}\tau^-\bar{\nu}_\tau)/\mathcal{B}(\bar{B}^0 \rightarrow D^{*+}\mu^-\bar{\nu}_\mu)$ ”. In: *Phys. Rev. Lett.* 115.11 (2015). [Erratum: *Phys.Rev.Lett.* 115, 159901 (2015)], p. 111803. DOI: [10.1103/PhysRevLett.115.111803](https://doi.org/10.1103/PhysRevLett.115.111803). arXiv: [1506.08614](https://arxiv.org/abs/1506.08614) [hep-ex].
- [16] R. Aaij et al. “Measurement of the ratio of the  $B^0 \rightarrow D^{*-}\tau^+\nu_\tau$  and  $B^0 \rightarrow D^{*-}\mu^+\nu_\mu$  branching fractions using three-prong  $\tau$ -lepton decays”. In: *Phys. Rev. Lett.* 120.17 (2018), p. 171802. DOI: [10.1103/PhysRevLett.120.171802](https://doi.org/10.1103/PhysRevLett.120.171802). arXiv: [1708.08856](https://arxiv.org/abs/1708.08856) [hep-ex].
- [17] R. Aaij et al. “Test of Lepton Flavor Universality by the measurement of the  $B^0 \rightarrow D^{*-}\tau^+\nu_\tau$  branching fraction using three-prong  $\tau$  decays”. In: *Phys. Rev. D* 97.7 (2018), p. 072013. DOI: [10.1103/PhysRevD.97.072013](https://doi.org/10.1103/PhysRevD.97.072013). arXiv: [1711.02505](https://arxiv.org/abs/1711.02505) [hep-ex].
- [18] Roel Aaij et al. “Test of lepton flavor universality using  $B^0 \rightarrow D^{*-}\tau^+\nu_\tau$  decays with hadronic  $\tau$  channels”. In: *Phys. Rev. D* 108.1 (2023), p. 012018. DOI: [10.1103/PhysRevD.108.012018](https://doi.org/10.1103/PhysRevD.108.012018). arXiv: [2305.01463](https://arxiv.org/abs/2305.01463) [hep-ex].
- [19] Yasmine Sara Amhis et al. “Averages of  $b$ -hadron,  $c$ -hadron, and  $\tau$ -lepton properties as of 2021”. In: *Phys. Rev. D* 107.5 (2023), p. 052008. DOI: [10.1103/PhysRevD.107.052008](https://doi.org/10.1103/PhysRevD.107.052008). arXiv: [2206.07501](https://arxiv.org/abs/2206.07501) [hep-ex].
- [20] Dante Bigi and Paolo Gambino. “Revisiting  $B \rightarrow D\ell\nu$ ”. In: *Phys. Rev. D* 94.9 (2016), p. 094008. DOI: [10.1103/PhysRevD.94.094008](https://doi.org/10.1103/PhysRevD.94.094008). arXiv: [1606.08030](https://arxiv.org/abs/1606.08030) [hep-ph].
- [21] Florian U. Bernlochner et al. “Combined analysis of semileptonic  $B$  decays to  $D$  and  $D^*$ :  $R(D^{(*)})$ ,  $|V_{cb}|$ , and new physics”. In: *Phys. Rev. D* 95.11 (2017). [Erratum: *Phys.Rev.D* 97, 059902 (2018)], p. 115008. DOI: [10.1103/PhysRevD.95.115008](https://doi.org/10.1103/PhysRevD.95.115008). arXiv: [1703.05330](https://arxiv.org/abs/1703.05330) [hep-ph].
- [22] Sneha Jaiswal, Soumitra Nandi, and Sunando Kumar Patra. “Extraction of  $|V_{cb}|$  from  $B \rightarrow D^{(*)}\ell\nu_\ell$  and the Standard Model predictions of  $R(D^{(*)})$ ”. In: *JHEP* 12 (2017), p. 060. DOI: [10.1007/JHEP12\(2017\)060](https://doi.org/10.1007/JHEP12(2017)060). arXiv: [1707.09977](https://arxiv.org/abs/1707.09977) [hep-ph].
- [23] Paolo Gambino, Martin Jung, and Stefan Schacht. “The  $V_{cb}$  puzzle: An update”. In: *Phys. Lett. B* 795 (2019), pp. 386–390. DOI: [10.1016/j.physletb.2019.06.039](https://doi.org/10.1016/j.physletb.2019.06.039). arXiv: [1905.08209](https://arxiv.org/abs/1905.08209) [hep-ph].
- [24] Marzia Bordone, Martin Jung, and Danny van Dyk. “Theory determination of  $\bar{B} \rightarrow D^{(*)}\ell^-\bar{\nu}$  form factors at  $\mathcal{O}(1/m_c^2)$ ”. In: *Eur. Phys. J. C* 80.2 (2020), p. 74. DOI: [10.1140/epjc/s10052-020-7616-4](https://doi.org/10.1140/epjc/s10052-020-7616-4). arXiv: [1908.09398](https://arxiv.org/abs/1908.09398) [hep-ph].
- [25] G. Martinelli, S. Simula, and L. Vittorio. “ $|V_{cb}|$  and  $R(D)^{(*)}$  using lattice QCD and unitarity”. In: *Phys. Rev. D* 105.3 (2022), p. 034503. DOI: [10.1103/PhysRevD.105.034503](https://doi.org/10.1103/PhysRevD.105.034503). arXiv: [2105.08674](https://arxiv.org/abs/2105.08674) [hep-ph].

- [26] Sebastien Descotes-Genon et al. “Optimizing the basis of  $B \rightarrow K^*\ell^+\ell^-$  observables in the full kinematic range”. In: *JHEP* 05 (2013), p. 137. DOI: [10.1007/JHEP05\(2013\)137](https://doi.org/10.1007/JHEP05(2013)137). arXiv: [1303.5794](https://arxiv.org/abs/1303.5794) [hep-ph].
- [27] Edward Witten. “Short Distance Analysis of Weak Interactions”. In: *Nucl. Phys. B* 122 (1977), pp. 109–143. DOI: [10.1016/0550-3213\(77\)90428-X](https://doi.org/10.1016/0550-3213(77)90428-X).
- [28] Gerhard Buchalla, Andrzej J. Buras, and Markus E. Lautenbacher. “Weak decays beyond leading logarithms”. In: *Rev. Mod. Phys.* 68 (1996), pp. 1125–1144. DOI: [10.1103/RevModPhys.68.1125](https://doi.org/10.1103/RevModPhys.68.1125). arXiv: [hep-ph/9512380](https://arxiv.org/abs/hep-ph/9512380).
- [29] Sebastien Descotes-Genon et al. “Implications from clean observables for the binned analysis of  $B \rightarrow K^*\mu^+\mu^-$  at large recoil”. In: *JHEP* 01 (2013), p. 048. DOI: [10.1007/JHEP01\(2013\)048](https://doi.org/10.1007/JHEP01(2013)048). arXiv: [1207.2753](https://arxiv.org/abs/1207.2753) [hep-ph].
- [30] R Aaij et al. “Measurement of Form-Factor-Independent Observables in the Decay  $B^0 \rightarrow K^{*0}\mu^+\mu^-$ ”. In: *Phys. Rev. Lett.* 111 (2013), p. 191801. DOI: [10.1103/PhysRevLett.111.191801](https://doi.org/10.1103/PhysRevLett.111.191801). arXiv: [1308.1707](https://arxiv.org/abs/1308.1707) [hep-ex].
- [31] A. Abdesselam et al. “Angular analysis of  $B^0 \rightarrow K^*(892)^0\ell^+\ell^-$ ”. In: (Apr. 2016). arXiv: [1604.04042](https://arxiv.org/abs/1604.04042) [hep-ex].
- [32] S. Wehle et al. “Lepton-Flavor-Dependent Angular Analysis of  $B \rightarrow K^*\ell^+\ell^-$ ”. In: *Phys. Rev. Lett.* 118.11 (2017), p. 111801. DOI: [10.1103/PhysRevLett.118.111801](https://doi.org/10.1103/PhysRevLett.118.111801). arXiv: [1612.05014](https://arxiv.org/abs/1612.05014) [hep-ex].
- [33] Morad Aaboud et al. “Angular analysis of  $B_d^0 \rightarrow K^*\mu^+\mu^-$  decays in  $pp$  collisions at  $\sqrt{s} = 8$  TeV with the ATLAS detector”. In: *JHEP* 10 (2018), p. 047. DOI: [10.1007/JHEP10\(2018\)047](https://doi.org/10.1007/JHEP10(2018)047). arXiv: [1805.04000](https://arxiv.org/abs/1805.04000) [hep-ex].
- [34] Albert M Sirunyan et al. “Measurement of angular parameters from the decay  $B^0 \rightarrow K^{*0}\mu^+\mu^-$  in proton-proton collisions at  $\sqrt{s} = 8$  TeV”. In: *Phys. Lett. B* 781 (2018), pp. 517–541. DOI: [10.1016/j.physletb.2018.04.030](https://doi.org/10.1016/j.physletb.2018.04.030). arXiv: [1710.02846](https://arxiv.org/abs/1710.02846) [hep-ex].
- [35] Bernat Capdevila et al. “Hadronic uncertainties in  $B \rightarrow K^*\mu^+\mu^-$ : a state-of-the-art analysis”. In: *JHEP* 04 (2017), p. 016. DOI: [10.1007/JHEP04\(2017\)016](https://doi.org/10.1007/JHEP04(2017)016). arXiv: [1701.08672](https://arxiv.org/abs/1701.08672) [hep-ph].
- [36] Marcel Algueró et al. “To (b)e or not to (b)e: no electrons at LHCb”. In: *Eur. Phys. J. C* 83.7 (2023), p. 648. DOI: [10.1140/epjc/s10052-023-11824-0](https://doi.org/10.1140/epjc/s10052-023-11824-0). arXiv: [2304.07330](https://arxiv.org/abs/2304.07330) [hep-ph].
- [37] M. Beneke and T. Feldmann. “Symmetry breaking corrections to heavy to light  $B$  meson form-factors at large recoil”. In: *Nucl. Phys. B* 592 (2001), pp. 3–34. DOI: [10.1016/S0550-3213\(00\)00585-X](https://doi.org/10.1016/S0550-3213(00)00585-X). arXiv: [hep-ph/0008255](https://arxiv.org/abs/hep-ph/0008255).
- [38] Sébastien Descotes-Genon et al. “On the impact of power corrections in the prediction of  $B \rightarrow K^*\mu^+\mu^-$  observables”. In: *JHEP* 12 (2014), p. 125. DOI: [10.1007/JHEP12\(2014\)125](https://doi.org/10.1007/JHEP12(2014)125). arXiv: [1407.8526](https://arxiv.org/abs/1407.8526) [hep-ph].
- [39] A. Khodjamirian et al. “Charm-loop effect in  $B \rightarrow K^{(*)}\ell^+\ell^-$  and  $B \rightarrow K^*\gamma$ ”. In: *JHEP* 09 (2010), p. 089. DOI: [10.1007/JHEP09\(2010\)089](https://doi.org/10.1007/JHEP09(2010)089). arXiv: [1006.4945](https://arxiv.org/abs/1006.4945) [hep-ph].

- [40] Nico Gubernari, Ahmet Kokulu, and Danny van Dyk. “ $B \rightarrow P$  and  $B \rightarrow V$  Form Factors from  $B$ -Meson Light-Cone Sum Rules beyond Leading Twist”. In: *JHEP* 01 (2019), p. 150. DOI: [10.1007/JHEP01\(2019\)150](https://doi.org/10.1007/JHEP01(2019)150). arXiv: [1811.00983](https://arxiv.org/abs/1811.00983) [hep-ph].
- [41] Marcel Algueró et al. “ $b \rightarrow s\ell^+\ell^-$  global fits after  $R_{K_S}$  and  $R_{K^{**}}$ ”. In: *Eur. Phys. J. C* 82.4 (2022), p. 326. DOI: [10.1140/epjc/s10052-022-10231-1](https://doi.org/10.1140/epjc/s10052-022-10231-1). arXiv: [2104.08921](https://arxiv.org/abs/2104.08921) [hep-ph].
- [42] Nico Gubernari, Danny van Dyk, and Javier Virto. “Non-local matrix elements in  $B_{(s)} \rightarrow \{K^{(*)}, \phi\}\ell^+\ell^-$ ”. In: *JHEP* 02 (2021), p. 088. DOI: [10.1007/JHEP02\(2021\)088](https://doi.org/10.1007/JHEP02(2021)088). arXiv: [2011.09813](https://arxiv.org/abs/2011.09813) [hep-ph].
- [43] Christoph Bobeth et al. “Long-distance effects in  $B \rightarrow K^*\ell\ell$  from analyticity”. In: *Eur. Phys. J. C* 78.6 (2018), p. 451. DOI: [10.1140/epjc/s10052-018-5918-6](https://doi.org/10.1140/epjc/s10052-018-5918-6). arXiv: [1707.07305](https://arxiv.org/abs/1707.07305) [hep-ph].
- [44] Nico Gubernari et al. “Dispersive Analysis of  $B \rightarrow K^{(*)}$  and  $B_s \rightarrow \phi$  Form Factors”. In: (May 2023). arXiv: [2305.06301](https://arxiv.org/abs/2305.06301) [hep-ph].
- [45] Thomas Blake et al. “An empirical model to determine the hadronic resonance contributions to  $\bar{B}^0 \rightarrow \bar{K}^{*0}\mu^+\mu^-$  transitions”. In: *Eur. Phys. J. C* 78.6 (2018), p. 453. DOI: [10.1140/epjc/s10052-018-5937-3](https://doi.org/10.1140/epjc/s10052-018-5937-3). arXiv: [1709.03921](https://arxiv.org/abs/1709.03921) [hep-ph].
- [46] Roel Aaij et al. “Angular Analysis of the  $B^+ \rightarrow K^{*+}\mu^+\mu^-$  Decay”. In: *Phys. Rev. Lett.* 126.16 (2021), p. 161802. DOI: [10.1103/PhysRevLett.126.161802](https://doi.org/10.1103/PhysRevLett.126.161802). arXiv: [2012.13241](https://arxiv.org/abs/2012.13241) [hep-ex].
- [47] R. Aaij et al. “Differential branching fractions and isospin asymmetries of  $B \rightarrow K^{(*)}\mu^+\mu^-$  decays”. In: *JHEP* 06 (2014), p. 133. DOI: [10.1007/JHEP06\(2014\)133](https://doi.org/10.1007/JHEP06(2014)133). arXiv: [1403.8044](https://arxiv.org/abs/1403.8044) [hep-ex].
- [48] Roel Aaij et al. “Measurements of the S-wave fraction in  $B^0 \rightarrow K^+\pi^-\mu^+\mu^-$  decays and the  $B^0 \rightarrow K^*(892)^0\mu^+\mu^-$  differential branching fraction”. In: *JHEP* 11 (2016). [Erratum: *JHEP* 04, 142 (2017)], p. 047. DOI: [10.1007/JHEP11\(2016\)047](https://doi.org/10.1007/JHEP11(2016)047). arXiv: [1606.04731](https://arxiv.org/abs/1606.04731) [hep-ex].
- [49] Roel Aaij et al. “Branching Fraction Measurements of the Rare  $B_s^0 \rightarrow \phi\mu^+\mu^-$  and  $B_s^0 \rightarrow f_2'(1525)\mu^+\mu^-$  Decays”. In: *Phys. Rev. Lett.* 127.15 (2021), p. 151801. DOI: [10.1103/PhysRevLett.127.151801](https://doi.org/10.1103/PhysRevLett.127.151801). arXiv: [2105.14007](https://arxiv.org/abs/2105.14007) [hep-ex].
- [50] W. G. Parrott, C. Bouchard, and C. T. H. Davies. “ $B \rightarrow K$  and  $D \rightarrow K$  form factors from fully relativistic lattice QCD”. In: *Phys. Rev. D* 107.1 (2023), p. 014510. DOI: [10.1103/PhysRevD.107.014510](https://doi.org/10.1103/PhysRevD.107.014510). arXiv: [2207.12468](https://arxiv.org/abs/2207.12468) [hep-lat].
- [51] Armen Tumasyan et al. “Measurement of the  $B_s^0 \rightarrow \mu^+\mu^-$  decay properties and search for the  $B^0 \rightarrow \mu^+\mu^-$  decay in proton-proton collisions at  $\sqrt{s} = 13$  TeV”. In: *Phys. Lett. B* 842 (2023), p. 137955. DOI: [10.1016/j.physletb.2023.137955](https://doi.org/10.1016/j.physletb.2023.137955). arXiv: [2212.10311](https://arxiv.org/abs/2212.10311) [hep-ex].
- [52] Siavash Neshatpour et al. “Neutral Current B-Decay Anomalies”. In: *Springer Proc. Phys.* 292 (2023), pp. 11–21. DOI: [10.1007/978-3-031-30459-0\\_2](https://doi.org/10.1007/978-3-031-30459-0_2). arXiv: [2210.07221](https://arxiv.org/abs/2210.07221) [hep-ph].

- [53] R. Aaij et al. “Measurement of lepton universality parameters in  $B^+ \rightarrow K^+\ell^+\ell^-$  and  $B^0 \rightarrow K^{*0}\ell^+\ell^-$  decays”. In: *Phys. Rev. D* 108.3 (2023), p. 032002. DOI: [10.1103/PhysRevD.108.032002](https://doi.org/10.1103/PhysRevD.108.032002). arXiv: [2212.09153](https://arxiv.org/abs/2212.09153) [hep-ex].
- [54] R. Aaij et al. “Test of lepton universality in  $b \rightarrow s\ell^+\ell^-$  decays”. In: *Phys. Rev. Lett.* 131.5 (2023), p. 051803. DOI: [10.1103/PhysRevLett.131.051803](https://doi.org/10.1103/PhysRevLett.131.051803). arXiv: [2212.09152](https://arxiv.org/abs/2212.09152) [hep-ex].
- [55] Benjamin Grinstein, Roxanne P. Springer, and Mark B. Wise. “Effective Hamiltonian for Weak Radiative  $B$  Meson Decay”. In: *Phys. Lett. B* 202 (1988), pp. 138–144. DOI: [10.1016/0370-2693\(88\)90868-4](https://doi.org/10.1016/0370-2693(88)90868-4).
- [56] Paolo Gambino, Martin Gorbahn, and Ulrich Haisch. “Anomalous dimension matrix for radiative and rare semileptonic  $B$  decays up to three loops”. In: *Nucl. Phys. B* 673 (2003), pp. 238–262. DOI: [10.1016/j.nuclphysb.2003.09.024](https://doi.org/10.1016/j.nuclphysb.2003.09.024). arXiv: [hep-ph/0306079](https://arxiv.org/abs/hep-ph/0306079).
- [57] Christoph Bobeth et al. “Complete NNLO QCD analysis of  $\bar{B} \rightarrow X_s\ell^+\ell^-$  and higher order electroweak effects”. In: *JHEP* 04 (2004), p. 071. DOI: [10.1088/1126-6708/2004/04/071](https://doi.org/10.1088/1126-6708/2004/04/071). arXiv: [hep-ph/0312090](https://arxiv.org/abs/hep-ph/0312090).
- [58] Mikolaj Misiak and Matthias Steinhauser. “NNLO QCD corrections to the  $\bar{B} \rightarrow X_s\gamma$  matrix elements using interpolation in  $m_c$ ”. In: *Nucl. Phys. B* 764 (2007), pp. 62–82. DOI: [10.1016/j.nuclphysb.2006.11.027](https://doi.org/10.1016/j.nuclphysb.2006.11.027). arXiv: [hep-ph/0609241](https://arxiv.org/abs/hep-ph/0609241).
- [59] Tobias Huber et al. “Electromagnetic logarithms in  $\bar{B} \rightarrow X_s\ell^+\ell^-$ ”. In: *Nucl. Phys. B* 740 (2006), pp. 105–137. DOI: [10.1016/j.nuclphysb.2006.01.037](https://doi.org/10.1016/j.nuclphysb.2006.01.037). arXiv: [hep-ph/0512066](https://arxiv.org/abs/hep-ph/0512066).
- [60] Tobias Huber, Tobias Hurth, and Enrico Lunghi. “Logarithmically Enhanced Corrections to the Decay Rate and Forward Backward Asymmetry in  $\bar{B} \rightarrow X_s\ell^+\ell^-$ ”. In: *Nucl. Phys. B* 802 (2008), pp. 40–62. DOI: [10.1016/j.nuclphysb.2008.04.028](https://doi.org/10.1016/j.nuclphysb.2008.04.028). arXiv: [0712.3009](https://arxiv.org/abs/0712.3009) [hep-ph].
- [61] Admir Greljo et al. “Rare  $b$  decays meet high-mass Drell-Yan”. In: *JHEP* 05 (2023), p. 087. DOI: [10.1007/JHEP05\(2023\)087](https://doi.org/10.1007/JHEP05(2023)087). arXiv: [2212.10497](https://arxiv.org/abs/2212.10497) [hep-ph].
- [62] Marco Ciuchini et al. “Constraints on lepton universality violation from rare B decays”. In: *Phys. Rev. D* 107.5 (2023), p. 055036. DOI: [10.1103/PhysRevD.107.055036](https://doi.org/10.1103/PhysRevD.107.055036). arXiv: [2212.10516](https://arxiv.org/abs/2212.10516) [hep-ph].
- [63] T. Hurth et al. “More Indications for Lepton Nonuniversality in  $b \rightarrow s\ell^+\ell^-$ ”. In: *Phys. Lett. B* 824 (2022), p. 136838. DOI: [10.1016/j.physletb.2021.136838](https://doi.org/10.1016/j.physletb.2021.136838). arXiv: [2104.10058](https://arxiv.org/abs/2104.10058) [hep-ph].
- [64] Marcel Algueró et al. “Are we overlooking lepton flavour universal new physics in  $b \rightarrow s\ell^+\ell^-$ ?” In: *Phys. Rev. D* 99.7 (2019), p. 075017. DOI: [10.1103/PhysRevD.99.075017](https://doi.org/10.1103/PhysRevD.99.075017). arXiv: [1809.08447](https://arxiv.org/abs/1809.08447) [hep-ph].
- [65] Marcel Algueró et al. “Emerging patterns of New Physics with and without Lepton Flavour Universal contributions”. In: *Eur. Phys. J. C* 79.8 (2019). [Addendum: *Eur.Phys.J.C* 80, 511 (2020)], p. 714. DOI: [10.1140/epjc/s10052-019-7216-3](https://doi.org/10.1140/epjc/s10052-019-7216-3). arXiv: [1903.09578](https://arxiv.org/abs/1903.09578) [hep-ph].

- [66] T. Hurth, F. Mahmoudi, and S. Neshatpour. “ $B$  anomalies in the post  $R_{K^{(*)}}$  era”. In: (Oct. 2023). arXiv: [2310.05585](https://arxiv.org/abs/2310.05585) [hep-ph].
- [67] David London and Joaquim Matias. “ $B$  Flavour Anomalies: 2021 Theoretical Status Report”. In: *Ann. Rev. Nucl. Part. Sci.* 72 (2022), pp. 37–68. doi: [10.1146/annurev-nucl-102020-090209](https://doi.org/10.1146/annurev-nucl-102020-090209). arXiv: [2110.13270](https://arxiv.org/abs/2110.13270) [hep-ph].
- [68] Johannes Albrecht, Danny van Dyk, and Christoph Langenbruch. “Flavour anomalies in heavy quark decays”. In: *Prog. Part. Nucl. Phys.* 120 (2021), p. 103885. doi: [10.1016/j.ppnp.2021.103885](https://doi.org/10.1016/j.ppnp.2021.103885). arXiv: [2107.04822](https://arxiv.org/abs/2107.04822) [hep-ex].
- [69] Nico Gubernari et al. “Improved theory predictions and global analysis of exclusive  $b \rightarrow s\mu^+\mu^-$  processes”. In: *JHEP* 09 (2022), p. 133. doi: [10.1007/JHEP09\(2022\)133](https://doi.org/10.1007/JHEP09(2022)133). arXiv: [2206.03797](https://arxiv.org/abs/2206.03797) [hep-ph].
- [70] B. Grzadkowski et al. “Dimension-Six Terms in the Standard Model Lagrangian”. In: *JHEP* 10 (2010), p. 085. doi: [10.1007/JHEP10\(2010\)085](https://doi.org/10.1007/JHEP10(2010)085). arXiv: [1008.4884](https://arxiv.org/abs/1008.4884) [hep-ph].
- [71] Bernat Capdevila et al. “Searching for New Physics with  $b \rightarrow s\tau^+\tau^-$  processes”. In: *Phys. Rev. Lett.* 120.18 (2018), p. 181802. doi: [10.1103/PhysRevLett.120.181802](https://doi.org/10.1103/PhysRevLett.120.181802). arXiv: [1712.01919](https://arxiv.org/abs/1712.01919) [hep-ph].
- [72] Eldar Ganiev. (On behalf of the Belle II Collaboration). Talk given at EPS-HEP 2023 “On Radiative and Electroweak Penguin Decays”, Hamburg, DESY. 2023.
- [73] Syuhei Iguro, Teppei Kitahara, and Ryoutaro Watanabe. “Global fit to  $b \rightarrow c\tau\nu$  anomalies 2022 mid-autumn”. In: (Oct. 2022). arXiv: [2210.10751](https://arxiv.org/abs/2210.10751) [hep-ph].
- [74] Andreas Crivellin et al. “Importance of Loop Effects in Explaining the Accumulated Evidence for New Physics in B Decays with a Vector Leptoquark”. In: *Phys. Rev. Lett.* 122.1 (2019), p. 011805. doi: [10.1103/PhysRevLett.122.011805](https://doi.org/10.1103/PhysRevLett.122.011805). arXiv: [1807.02068](https://arxiv.org/abs/1807.02068) [hep-ph].
- [75] Marcel Algueró et al. “Disentangling lepton flavor universal and lepton flavor universality violating effects in  $b \rightarrow s\ell^+\ell^-$  transitions”. In: *Phys. Rev. D* 105.11 (2022), p. 113007. doi: [10.1103/PhysRevD.105.113007](https://doi.org/10.1103/PhysRevD.105.113007). arXiv: [2205.15212](https://arxiv.org/abs/2205.15212) [hep-ph].
- [76] Aritra Biswas et al. “A new puzzle in non-leptonic  $B$  decays”. In: *JHEP* 06 (2023), p. 108. doi: [10.1007/JHEP06\(2023\)108](https://doi.org/10.1007/JHEP06(2023)108). arXiv: [2301.10542](https://arxiv.org/abs/2301.10542) [hep-ph].